Singular Spectrum Analysis of Traffic Workload in a Large-Scale Wireless LAN [*]

George Tzagkarakis, Maria Papadopouli and Panagiotis Tsakalides

Department of Computer Science, University of Crete &
Institute of Computer Science, Foundation for Research and Technology-Hellas
P.O. Box 1385, 711 10 Heraklion, Crete, Greece
{gtzag, mgp, tsakalid}@ics.forth.gr

ABSTRACT

Network traffic load in an IEEE802.11 infrastructure arises from the superposition of traffic accessed by wireless clients associated with access points (APs). An accurate characterization of these data can be beneficial in modelling network traffic and addressing a variety of problems including coverage planning, resource reservation and network monitoring for anomaly detection. This study focuses on the statistical analysis of the traffic load measured in a campus-wide IEEE802.11 infrastructure at each AP.

Using the Singular Spectrum Analysis approach, we found that the time-series of traffic load at a given AP has a small intrinsic dimension. In particular, these time-series can be accurately modelled using a small number of leading (principal) components. This proved to be critical for understanding the main features of the components forming the network traffic.

The statistical analysis of leading components has demonstrated that even a few first components form the main part of the information. The residual components capture the small irregular variations, which do not fit in the basic part of the network traffic and can be interpreted as a stochastic noise. Based on these properties, we also studied contributions of the various components to the overall structure of the traffic load of an AP and its variation over time.

Categories and Subject Descriptors

C.2.3 [**Computer-Communication Networks**]: Network operations; I.6.6 [**Model Development**]: Modelling methodologies

General Terms

Algorithms, measurement, performance, experimentation.

Keywords

Wireless traffic modelling, singular spectrum analysis.

1. INTRODUCTION

Wireless networks are increasingly being deployed to provide Internet access in airports, universities, corporations, hospitals, residential, and other public areas. Furthermore, there is a growth in peer-to-peer, streaming, and VoIP traffic over the wireless infrastructures [1, 2]. At the same time, empirical studies and performance analysis indicate dramatically low performance of real-time constrained applications over Wireless Local Area Networks (WLANs) [3]. WLANs have more vulnerabilities and bandwidth/latency constrains than their wired counterparts. The bandwidth utilization at an AP can impact the performance of the wireless clients in terms of throughput, delay, and energy consumption. For quality of service provision, capacity planning, load balancing, and network monitoring, it is critical to understand the traffic characteristics. For this purpose, the design of accurate models of the network and client activity are critical. In addition, the traffic models can assist in detecting abnormal traffic patterns (e.g., due to malicious attacks, AP or client misconfigurations and failures).

One of the most intriguing aspects of the traffic demand modelling in WLANs is its intrinsic multi-level, spatio-temporal nature, namely, the different spatial scales (e.g., infrastructure-wide, AP-level or client-level) and time granularities, such as packet-level, flow-level and session-level. While there is a rich literature characterizing traffic in wired networks [4, 5, 6], there are only a few studies available examining wireless traffic load. In a recent work [7, 8], two key structures in a WLAN, namely, the session of a client and the traffic flows generated within that session by that client, were modelled in both spatial and temporal dimensions, and their dependencies and interrelations were examined. In [9, 10], the traffic load at APs was modelled using variants of the Moving Average and Autoregressive Moving Average models, resulting in simple forecasting methods. This paper extends these research efforts by focusing on the statistical modelling of the wireless traffic load at the AP-level, from a spatial scale point of view, and using packet-level time granularity. To the best of our knowledge, this is the first

[*] This work was supported by the Greek General Secretariat for Research and Technology under programs ΠΕΝΕΔ-Code 03ΕΔ69, Crete Wise KP-18, and 05NON-EU-238, and the European Commission under programs MIRG-CT-2005-029186 and MTKD-CT-2005-029791.

MSWIM'07, October 22–26, 2007, Chania, Crete Island, Greece.
Copyright 2007 ACM 978-1-59593-851-0/07/0010 ...$5.00.

study in characterizing statistically wireless traffic load at this spatio-temporal scale using non-linear time-series analysis techniques.

Here, we study a large-scale wireless infrastructure [11] using a lightweight data acquisition methodology. Our data was collected using the Simple Network Management Protocol (SNMP), the most widely-available monitoring service in wireless platforms. Any AP in the market supports monitoring using SNMP, so it is important to understand how much operators and researchers can learn from SNMP data. Furthermore, this type of data is the most appropriate one to understand daily and long-term trends in the usage of wireless networks. This paper makes use of SNMP data for analyzing traffic characteristics, such as total load and periodicities.

To achieve a deeper understanding of the main features of traffic measurements, we employ a non-linear time-series analysis [12]. At the same time, due to the complicated structure of a traffic series, traditional algorithms of non-linear analysis may not estimate reliably the analyzed time-series. However, after filtering out a high-frequency component, which can be considered as a noisy part, we expect to obtain a more accurate estimation of the embedding dimension of the underlying process. Motivated by this observation, in this study, we analyze traffic series by decomposing them in two components, namely, a low-frequency and a high-frequency one, using Singular Spectrum Analysis (SSA).

The Principal Component Analysis (PCA) [13] consists in applying a linear transformation of the original data space into a feature space, where the data set may be represented by a reduced number of "effective" features, while retaining most of the information content of the data. The SSA [14] belongs to the general category of PCA methods and is very efficient for the analysis of time-series corresponding to an arbitrary process. In a recent work [15], the SSA was used to analyze the dynamics of traffic obtained at an intermediate-scale wired LAN. To the best of our knowledge, this is the first study that applies SSA on the analysis of traffic from a WLAN.

This paper employs SSA to explore the intrinsic dimensionality and structure of the time-series corresponding to the traffic load at a given AP, using data collected from a campus-wide WLAN infrastructure. To explore the nature of this dimensionality, we introduce the notion of *eigenloads*. Derived from the implementation of SSA on a given traffic load series, an eigenload is a time-series that captures a particular source of temporal variability. Each traffic load series can be expressed as a weighted sum of eigenloads, where the weights are proportional to the extend to which each eigenload is present in the given traffic load series.

We show that traffic eigenloads in a WLAN fall into two natural classes; namely, *deterministic eigenloads*, which capture the slow-varying trends in the traffic load series, and *noise eigenloads*, which account for traffic fluctuations appearing to have relatively time-invariant properties. By categorizing eigenloads in this manner, we obtain a significant insight into the intrinsic properties of the traffic load series. In particular, we find that each time-series can be well approximated by only a small number of eigenloads, which constitute its "feature set". Furthermore, these features vary in a predictable way as a function of the amount of traffic carried in the time-series. We show that the largest traffic load series, i.e., the series with the highest mean traffic load, are primarily deterministic. On the other hand, traffic load series of moderate size are generally comprised of noisy features.

The paper is organized as follows: Section 2, describes the wireless infrastructure at the University of North Carolina at Chapel Hill (UNC) and the data acquisition process. In Section 3, we present the basic concept of the SSA approach. We apply this method on our traffic measurements and analyze the leading components, which are responsible for the main part of the network's traffic, and the residual components, which can be represented as irregular variations of the data. Section 4, provides a statistical modelling for a set of traffic load series, and then applies SSA to these time-series and presents the low-dimensionality property. Section 5, presents the classification of the eigenloads in two classes, and focuses on the characteristics of the decomposition of traffic load series into their constituent eigenloads. Finally, in Section 6, we summarize our main results and discuss future work plans.

2. BACKGROUND

The IEEE802.11 infrastructure at UNC provides coverage for the 729-acre campus and a number of off-campus administrative offices. The university has 26.000 students, 3.000 faculty members and 9.000 staff members. Undergraduate students (16.000) are required to own laptops, which are generally able to communicate using the campus wireless network. A total of 488 APs were part of the campus network at the start of our study. These APs belong to three different series of the Cisco Aironet platform: the state-of-the-art 1210 Series (269 APs), the widely deployed 350 Series (188 APs) and the older 340 Series (31 APs).

The data was collected using SNMP for polling every AP on campus every five minutes. First, the system was implemented using a nonblocking SNMP library for polling each AP precisely every five minutes in an independent manner. This eliminates any extra delays due to the slow processing of SNMP polls by some of the slower APs. The system ran in a multiprocessor system and the CPU utilization in each of the three processors we employed never exceeded 70%. Second, our characterization of the workload of the APs is derived only from those clients associated with the AP at polling time.

The data collection took place between 9:09 a.m. September 29th, 2004 and 12:00 a.m. November 30th, 2004. The total number of polling operations during the 63 days was 8.247.479. The data collection system ran flawlessly for the entire period, but APs were sometimes unresponsive. This is generally due to maintenance down-times, reboots, or overloads. If an AP did not respond to a poll, the data collection system tried again 5 *sec* later (and if necessary, again after 10 *sec* and 15 *sec*). It is therefore unlikely that datagram losses created holes in our dataset.

Based on the SNMP trace for each AP, we produced a time series of its traffic load at hourly intervals. This traffic is the total amount of bytes received and sent from all clients that were associated with the AP at that time interval. In the rest of the paper, depending on the mathematical expression, we will use two notations for these time series. Specifically, the traffic of the AP i during the h-th hour of day d ($h \in \{1, \ldots, 24\}$, $d \in \{1, \ldots, 63\}$), that corresponds to time t, is $T_i(h, d) = X_i(t)$.

3. SINGULAR SPECTRUM ANALYSIS OF A TIME-SERIES

Singular Spectrum analysis (SSA) is a method suitable for extracting information from short and noisy time series. It unravels the information embedded in the delay-coordinate phase space by decomposing the sequence into elementary patterns of behavior in time and spectral domains, that help separating the time series into statistically independent components, which can be classified as trends and deterministic oscillations (or noise). SSA looks for structures in a time series by doing an eigendecomposition of the so-called lagged covariance matrix. This approach is useful in non-linear system analysis, because, as opposed to other time-series analysis techniques, we do not have to choose the structure functions *a priori*, but instead, the data lets themselves to choose the temporal structures.

Time-series corresponding to wireless traffic load are often short and contain typically peaks on top of a more regular background. Besides, these series often have both regular (periodic) and irregular (noisy) aspects, which may be present in different spatial and temporal scales. Thus, the need for combining a deterministic with a stochastic modelling approach is necessary, motivating the use of the SSA approach. In the following, we describe the modelling process step by step, and apply it on randomly selected time-series corresponding to several hotspot APs of our dataset.

3.1 Introduction to SSA

The SSA is applied to the analysis of time-series corresponding to an arbitrary signal $x(t)$, with $t > 0$. The standard SSA consists of four main steps:

1. Transformation of the one-dimensional time-series into a trajectory (Hankel) matrix;

2. Singular Value Decomposition (SVD) of the Hankel matrix;

3. PCA and selection of the dominant features by grouping the SVD components;

4. Reconstruction of the original time-series using the selected features (inverse Hankelization by diagonal averaging).

Let $X = \{x_j\}_{j=1}^N$ denote the samples of the time-series and L $(1 < L < N)$ be an integer, indicating the (caterpillar) window length. The transformation step forms $K = N-L+1$ lagged vectors $X_k = \{x_k, \ldots, x_{k+L-1}\}^T$, $1 \leq k \leq K$. The trajectory Hankel matrix of the time-series X is of dimension $L \times K$ and has the following form:

$$\mathbf{H} = [X_1 \; X_2 \; \cdots \; X_K] \; . \tag{1}$$

The trajectory space is defined as the linear space spanned by the columns of $\mathbf{H}$.

After the above Hankelization process, the SSA method performs an SVD of the matrix $\mathbf{C} = \mathbf{H}\mathbf{H}^T$. Let $\lambda_1 \geq \ldots \geq \lambda_L$ be the eigenvalues of $\mathbf{C}$, which give the energy attributable to the respective principal component, and $r = \max\{i : \lambda_i > 0\}$. Let $U_1, \ldots, U_r$ denote the corresponding eigenvectors (principal components) and $V_j = \mathbf{H}^T U_j / \sqrt{\lambda_j}$, $j = 1, \ldots, r$, the set of factor vectors, which capture the temporal variation common to all lagged vectors along the j-th principal axis. We refer to the set $\{V_j\}_{j=1}^r$ as the set of *eigenloads* of X. Since the principal axes are in order of contribution to the overall energy, V_1 captures the strongest temporal trend common to all lagged vectors, V_2 captures the next strongest trend and so on. If we denote $\mathbf{H}_j = \sqrt{\lambda_j} U_j V_j^T$, the trajectory matrix $\mathbf{H}$ can be written as

$$\mathbf{H} = \mathbf{H}_1 + \cdots + \mathbf{H}_r \; . \tag{2}$$

By applying the inverse Hankelization process on each matrix $\mathbf{H}_j$, we obtain an approximation X^j of the original series X.

Once the expansion given by (2) has been completed, the third step of the SSA method consists of partitioning the set of indices $\mathcal{I} = \{1, \ldots, r\}$ into s disjoint subsets, where the value of s depends on the specific application. Let $\mathcal{I}_1 = \{i_1, \ldots, i_m\}$ be the first subset of indices, and $\mathbf{H}^{\mathcal{I}_1} = \mathbf{H}_{i_1} + \cdots + \mathbf{H}_{i_m}$ to be the approximation of the trajectory matrix $\mathbf{H}$ based on the indices of $\mathcal{I}_1$. Similarly, we have an analogous decomposition corresponding to each subset $\mathcal{I}_k$, $k = 2, \ldots, s$. Thus, we obtain the final decomposition of the initial Hankel matrix $\mathbf{H}$:

$$\mathbf{H} = \mathbf{H}^{\mathcal{I}_1} + \cdots + \mathbf{H}^{\mathcal{I}_s} \; . \tag{3}$$

The last step of the SSA is the application of an inverse Hankelization process on the approximation matrix $\mathbf{H}^{\mathcal{I}_k}$, $k = 1, \ldots, s$, to approximate the initial time-series. This process is simply performed by averaging the elements of $\mathbf{H}^{\mathcal{I}_k}$, which are placed on the same anti-diagonal, that is, the elements $h_{ij}^{\mathcal{I}_k}$ with $i + j =$ constant. Let $X^{\mathcal{I}_k}$ denote the time-series reconstructed using the matrix $\mathbf{H}^{\mathcal{I}_k}$. Then, the j-th component of $X^{\mathcal{I}_k}$, $x_j^{\mathcal{I}_k}$, is given by: $x_j^{\mathcal{I}_k} =$ mean{elements of $\mathbf{H}^{\mathcal{I}_k}$ which are placed on the j-th anti-diagonal}[1]. Thus, the result of SSA is an expansion of the original time-series into a sum of s series,

$$X = X^{\mathcal{I}_1} + \cdots + X^{\mathcal{I}_s} \; , \tag{4}$$

where $X^{\mathcal{I}_k}$ is the time-series reconstructed using the matrix $\mathbf{H}^{\mathcal{I}_k}$. For instance, the case $s = 2$ can be interpreted as a problem of separating a signal from a noise component. The performance of the method mainly depends on two parameters, namely, the selection of the window length L and the partitioning of the positive eigenvalues. In the following, we describe procedures for the specification of these parameters, when using SSA for WLAN traffic workload analysis.

3.2 Estimation of the window length L

The selection of a suitable window length, L, is crucial for an increased accuracy of the SSA. The value of L is computed, such that the points of different lagged vectors, X_k, X_l $(k \neq l)$, can be considered as linearly independent. In our context, for an arbitrary AP, the window length L is chosen to be equal to the correlation length (time lag), i.e., when the sample auto-correlation function

$$C(L) = \frac{\sum_{j=1}^N (x_{j+L} - \bar{x})(x_j - \bar{x})}{\sum_{j=1}^N (x_j - \bar{x})^2} \; , \tag{5}$$

crosses for the first time the confidence interval corresponding to the white Gaussian noise. In this case, the lagged vectors of length L can be considered to be independent, which enables each vector to be analyzed separately. In (5), $\bar{x}$ denotes the arithmetic mean of the time-series X.

[1] The first anti-diagonal is simply the element $h_{11}^{\mathcal{I}_k}$.

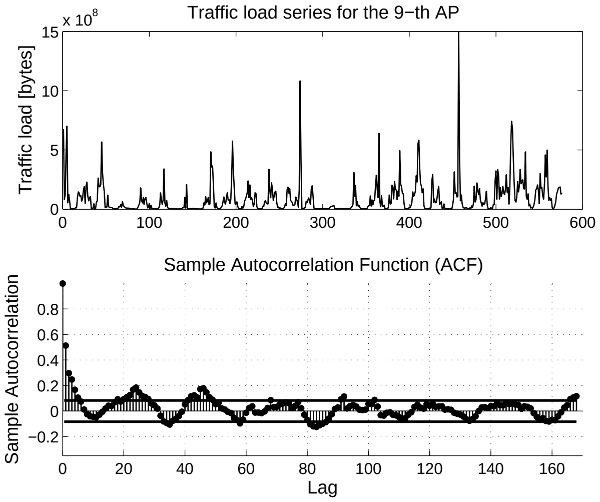

Figure 1: Traffic load series and sample auto-correlation function for $X_9(t)$.

Fig. 1 presents the traffic load series and the values of the sample auto-correlation function as a function of the window length L (time lag), together with the confidence interval corresponding to the white Gaussian noise, for an AP of our dataset. As shown, the auto-correlation function first crosses the confidence interval for $L = 7$, that is, the selected window length should be equal to 7.

In the following two subsections, we describe the procedure for partitioning the set of the r eigentriples $\{\lambda_j, U_j, V_j\}_{j=1}^r$ into s disjoint subsets. For convenience, we focus on the case $s = 2$, that is, the eigentriples are divided in two classes, namely, the principal and the residual eigentriples.

3.3 Analysis of leading components

As it was mentioned before, the eigenvalues given by applying an SVD on the trajectory matrix $\mathbf{H}$ can be used to select a set of *feature components* for the reconstruction of the original time-series. In particular, the ratio

$$R_i = \frac{\lambda_i}{\sum_{j=1}^{L} \lambda_j} \tag{6}$$

is used to estimate the energy contribution (in decreasing order) of the i-th principal component in the analyzed time-series, which can be represented as the fraction of the information content related to that (single) component.

Fig. 2 shows the contribution of the eigenvalues corresponding to the traffic series of the 9-th AP in our dataset, for two different window lengths, namely, the window length $L_1 = 7$ given by the auto-correlation function (5), and $L_2 = 14$. This information permits the estimation of the number of principal components which effectively contribute to the information content of the time-series. As it can be seen, only the first few principal components are responsible for the main part of the traffic information, that is, the part that maintains a high energy content.

For simplicity, we are interested in grouping the principal components in two subsets, namely, a subset $\mathcal{I}_1$, containing the eigenvalues which are responsible for the reconstruction of a slow varying (trend) component of the original time-series, and a subset $\mathcal{I}_2$, which is related to its "noisy" part. In the standard SSA approach, this partition is performed based on a signal processing point of view. In particular, the subset $\mathcal{I}_1$ consists of the eigenvalues λ_j whose corresponding eigenvectors U_j have slow varying sequences of elements, that is, the contribution of harmonics with *low frequencies* into their Fourier expansion is high. Similarly, the subset $\mathcal{I}_2$ consists of those eigenvalues, for which the contribution of harmonics with *high frequencies* into the Fourier expansion of their corresponding eigenvectors is high. In both cases, the contribution can be measured using the periodogram [16] of each eigenvector.

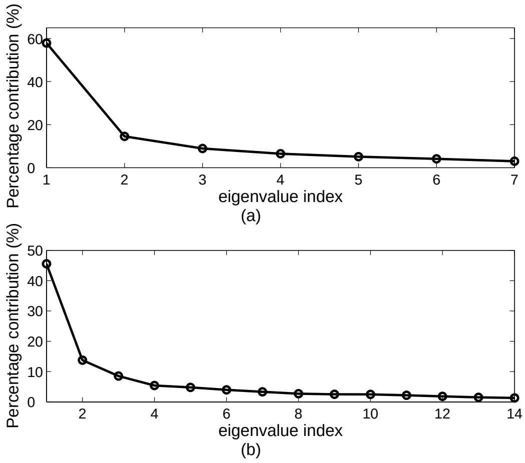

Figure 2: Percentage contribution of the eigenvalues for $X_9(t)$: (a) $L = 7$, (b) $L = 14$.

In our study, instead of following this procedure, the partition of the eigenvalues is based on a statistical criterion, in order to take into account the uncertainty of the underlying statistical model. In particular, the subset $\mathcal{I}_1$ of principal components will consist of those eigenvalues for which the reconstructed time-series has a statistical distribution of the traffic measurements similar to the distribution of the original time-series. Let $p(x)$ denote the probability density function (PDF), which best fits the traffic load series of a given AP. Then, a leading component belongs to $\mathcal{I}_1$, if the PDF of the corresponding reconstructed series, $\hat{p}(x)$, is close to $p(x)$, where the "closeness" is measured using the χ^2 test [17]. In this case, the null hypothesis tested by the χ^2 test is that the distribution of the series which is reconstructed using the first l $(1 \leq l \leq L)$ principal components, is modelled with $p(x)$.

As an illustration, Fig. 3 shows the value of the χ^2 test as a function of the number l of the first principal components, for the series $X_9(t)$, whose distribution is best fitted by a Weibull PDF, as it will be described in more detail in Section 4. We used a window size ($L = 14$), which is larger than the "optimal" ($L = 7$), in order to better visualize the variability of the χ^2 test. The two parallel lines correspond to the significance levels[2] $\alpha = 0.1$ (top line) and $\alpha = 0.9$ (bottom line). For instance, the distribution of the reconstructed series does not pass the null hypothesis (that is,

[2] The significance level indicates the probability that the estimated χ^2 value will exceed the theoretical χ^2 value by chance even for a correct model.

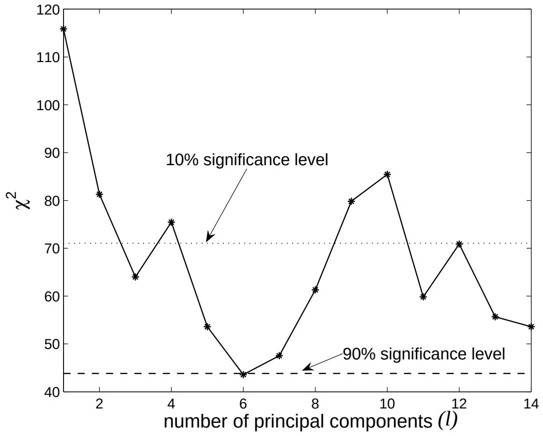

Figure 3: The value of χ^2 as a function of the number l of leading components for $X_9(t)$ analyzed with $L = 14$.

it cannot be modeled as a Weibull PDF), when the reconstruction is based only on the first leading component, since the corresponding χ^2 value is out of the confidence interval (parallel lines). On the other hand, as l increases the value of χ^2 decreases, and for $l = 5$, there is already a quite good level of correspondence of the distribution of the reconstructed series, using the first 5 leading components, to the null hypothesis. This is important, since only the first 5 components contain the main part of the original time-series. Notice that the statistical criterion is consistent with an energy-based rule, i.e., the first five components satisfying the χ^2 test, also contain a high portion ($\approx 80\% = \sum_{i=1}^{5} R_i$) of the total energy of the original series.

3.4 Analysis of residual components

As it was mentioned before, the influence of the residual components, corresponding to the smallest eigenvalues of the trajectory matrix is related to small irregular variations that do not fit in the basic model of the traffic load and can be interpreted as stochastic noise. As an illustration, Fig. 4 presents the time-series reconstructed on the basis of the smallest residual component of the original series $X_9(t)$, using the window length ($L = 7$) given by the sample autocorrelation function. This time-series has a significantly different structure compared to its original version. Its distribution approximates a Gaussian density, as the qq-plot test in Fig. 5 shows. Notice that this reconstructed series does not represent physical traffic load, since it takes negative values.

However, when increasing the number of residual components, their distribution starts losing its initial form, together with an increase of the correlations between the series samples. Fig. 6 shows the value of the χ^2 test as a function of the number of *residual* components l ($1 \leq l \leq L$), that is, the first l residual components corresponding to the first l *smallest* eigenvalues, together with the two significance levels ($\alpha = 0.1$–top line, $\alpha = 0.9$–bottom line).

To select the residual components (elements of the $\mathcal{I}_2$ subset), we employ the instance where the symmetry of the distribution of the reconstructed time-series using the first l residual components (smallest eigenvalues) is violated. It can be seen that χ^2 exceeds the 10% ($\alpha = 0.1$) significance level when the number of residual components is equal to $l = 6$. Thus, the subset $\mathcal{I}_2$ contains the first $l - 1 = 5$ smallest (non-zero) eigenvalues.

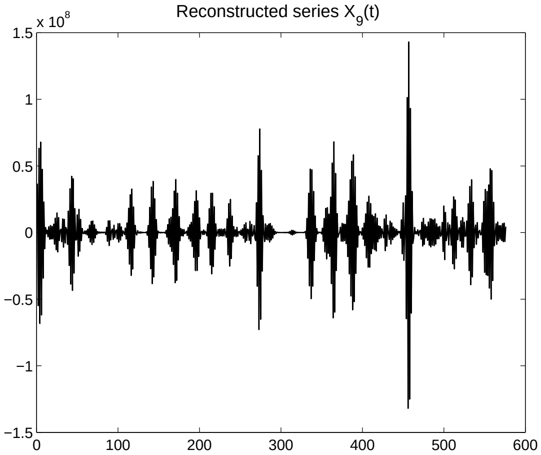

Figure 4: The series $X_9(t)$ reconstructed using the smallest residual component, for a window length $L = 7$.

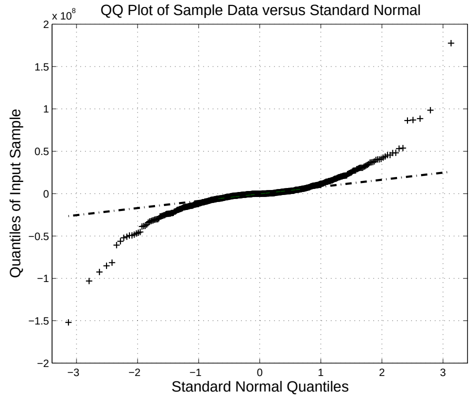

Figure 5: Quantile-Quantile plot of the reconstructed series $X_9(t)$ using the smallest residual component, for a window length $L = 7$.

Following the analysis described in previous sections, we constructed two subsets of eigenvalues, namely, subset $\mathcal{I}_1$ containing the leading components, and subset $\mathcal{I}_2$ containing the residual components of the trajectory matrix $\mathbf{H}$ for a given time-series $X(t)$. Notice that in general $(\mathcal{I}_1 \cup \mathcal{I}_2) \subseteq \mathcal{I}$, that is, the analysis of the leading and residual components may not result in an exact partitioning of the initial set of eigenvalues, $\mathcal{I}$, since there are eigenvalues that may not belong in any of the two subsets. Thus, we should replace the equation in (3) (for $s = 2$) by an approximation

$$\mathbf{H} \approx \mathbf{H}^{\mathcal{I}_1} + \mathbf{H}^{\mathcal{I}_2} \ . \qquad (7)$$

The application of diagonal averaging (inverse Hankelization) on both sides of (7) results in the following approximation of the original time-series:

$$X(t) \approx X^{\mathcal{I}_1}(t) + X^{\mathcal{I}_2}(t) \ , \qquad (8)$$

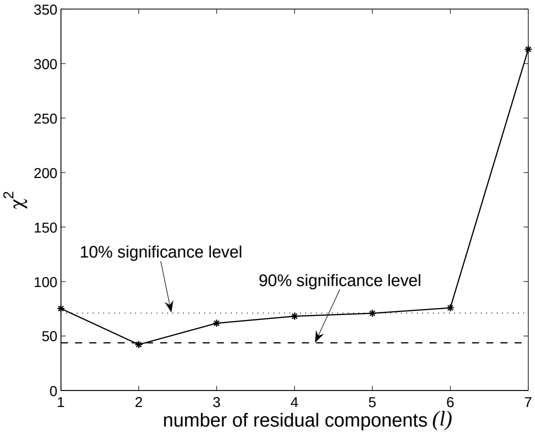

Figure 6: The value of χ^2 as a function of the number l of residual components for $X_9(t)$ analyzed with $L = 7$.

where $X^{\mathcal{I}_1}(t)$ is the time-series reconstructed using the subset of leading components, which can be interpreted as the trend of $X(t)$, and $X^{\mathcal{I}_2}(t)$ is the time-series reconstructed using the subset of residual components, which can be interpreted as the "noisy" (high-frequency) part of $X(t)$.

4. SSA-BASED TRAFFIC LOAD SERIES MODELLING AND DECOMPOSITION

As discussed in Section 3, we aim in applying the SSA to decompose the traffic load series of a given AP into its constituent set of eigenloads. Besides, Section 3.3 maintained that the determination of the most important (leading) eigenloads is based on the selection of a suitable statistical model, which accurately fits the distribution of the original traffic load series, to be used in the χ^2 test. Thus, a statistical analysis for the selection of the best model is necessary.

This section first shows that traffic load series corresponding to different APs can be modelled using PDFs belonging to different families. Then, we use the corresponding best models to show that only a small set of eigenloads can reconstruct the original time-series accurately, while preserving its characteristic features, such as its spikes.

4.1 Statistical modelling of traffic load series

The first step in our statistical analysis is based on accurate modelling of the mode and tails of the distribution of a given traffic load series. Since the time-series in our dataset are in general bursty, we expect that their distributions will be modelled using non-Gaussian PDFs. Before proceeding, we assess whether the data deviate from the normal distribution using qq-plots. Then, we determine the model that best fits the empirical distribution of the time-series by employing the so-called amplitude probability density (APD) curves, which represent the probability $P(|X| > x)$. The APD curves give a good indication of whether or not a particular PDF $p(x)$ matches our data near the mode and on the tails of the empirical distribution.

Table 1 indicates the candidate statistical models used in our analysis. The statistical fitting of each one of the 19 time-series constituting our dataset showed that the Gamma is the dominant distribution followed by the GGD. Fig. 7 shows the APD curves for the traffic load series $X_2(t)$ and $X_5(t)$, whose empirical distribution is best approximated using the GGD and Gamma distribution, respectively.

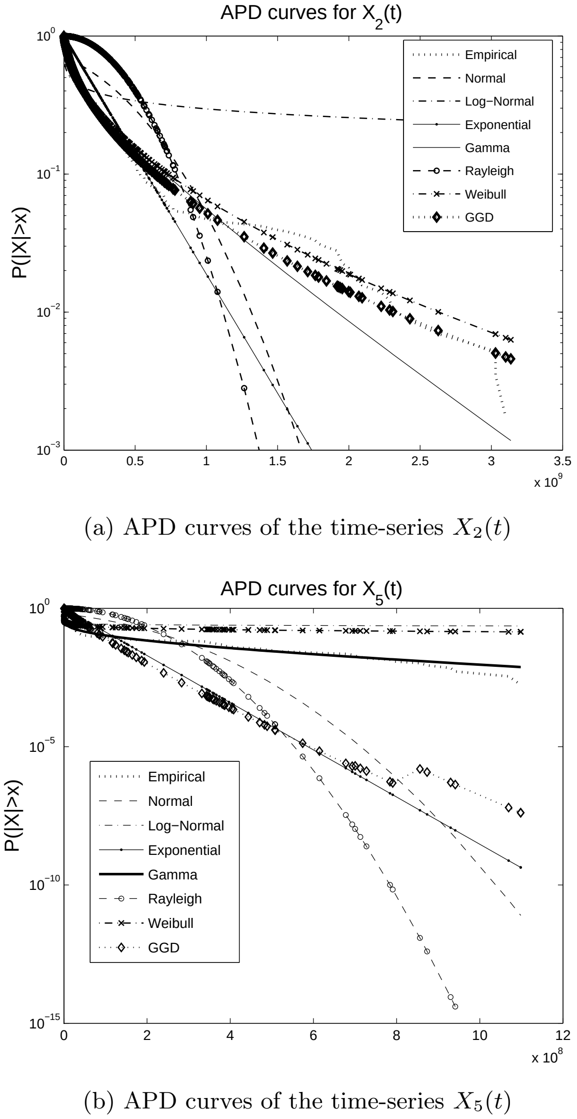

(a) APD curves of the time-series $X_2(t)$

(b) APD curves of the time-series $X_5(t)$

Figure 7: APD curves for the time-series corresponding to the APs: (a) $X_2(t)$, (b) $X_5(t)$.

4.2 Normalization of the traffic measurements

Due to the nature of wireless traffic, the traffic load of a particular AP i within hour t, $X_i(t)$, exhibits spikes that are very hard to predict. Fig. 8 shows the traffic load series and its normal probability plot for the third hotspot AP in our dataset, $X_3(t)$. Its bursty behavior is clear, and the marginal distribution is non-Gaussian. Thus, before proceeding to handle the data more efficiently, we normalize them (i.e., resemble a normal distribution), by employing a suitable transformation. Such distributions can be handled more effectively. Besides, such a transformation can reduce the effect of those high local spikes on the forecasting per-

Table 1: The models used in the traffic load series analysis.

Model	PDF
Normal	$p(x) = \frac{1}{\sigma\sqrt{2\pi}} e^{-(x-\mu)^2/(2\sigma^2)}$
log-Normal	$p(x) = \frac{1}{x\sigma\sqrt{2\pi}} e^{-(\ln x-\mu)^2/(2\sigma^2)},\ x \in (0,\infty)$
Exponential	$p(x) = \frac{1}{\mu} e^{-x/\mu}$
Gamma	$p(x) = \frac{1}{b^\alpha\,\Gamma(\alpha)} x^{\alpha-1} e^{-x/b},\ x \in [0,\infty)$
Rayleigh	$p(x) = \frac{x}{b^2} e^{-x^2/(2b^2)},\ x \in [0,\infty)$
Weibull	$p(x) = b\alpha^{-b} x^{b-1} e^{-(x/\alpha)^b},\ x \in [0,\infty)$
Generalized Gaussian density (GGD)	$p(x) = \frac{b}{2\alpha\,\Gamma(1/b)} e^{-(\lvert x\rvert/\alpha)^b}$

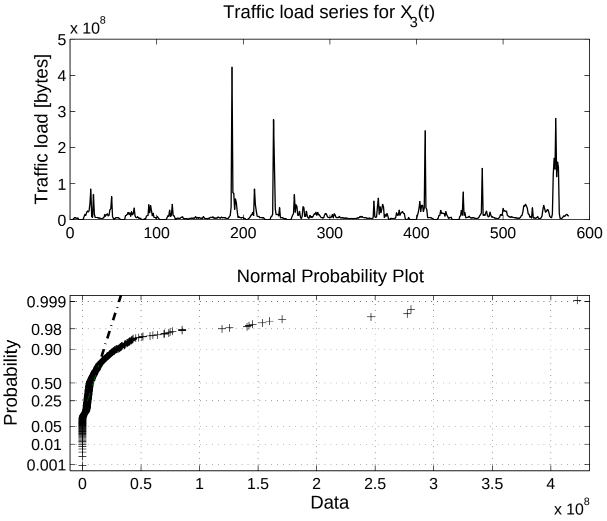

Figure 8: Traffic load series and normal probability plot for $X_3(t)$.

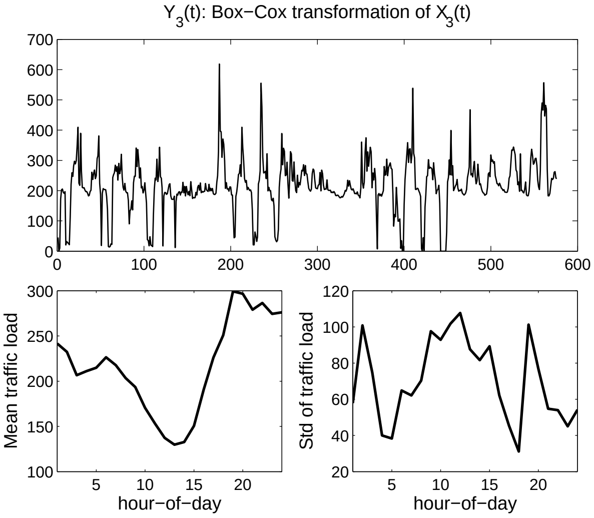

Figure 9: Box-Cox transformation of $X_3(t)$ (upper figure) and the patterns of the mean and standard deviation per hour-of-day of the original traffic load.

formance. Unfortunately, in general, the choice of the best transformation is not obvious.

There is a family of power transformations to make the marginal distributions resemble a Gaussian-like density, namely the Box-Cox power transformations, defined only for positive data values. The existence of zero values in the trace does not pose any problem, since a constant can always be added. The Box-Cox power transformation is given by [18]:

$$x(\rho) = \begin{cases} \frac{x^\rho - 1}{\rho}, & \rho \neq 0 \\ \ln(x), & \rho = 0 \end{cases} \tag{9}$$

Given the time-series $X = \{x_j\}_{j=1}^N$, one way to select the optimal power ρ is to maximize the log-likelihood function

$$f(X,\rho) = -\frac{N}{2}\ln\Big[\sum_{j=1}^{N}\frac{(x_j(\rho)-\bar{x}(\rho))^2}{N}\Big] + (\rho-1)\sum_{j=1}^{N}\ln(x_j(\rho))\ , \tag{10}$$

where

$$\bar{x}(\rho) = \frac{1}{N}\sum_{j=1}^{N} x_j(\rho)\ .$$

Let $Y_i(t) = X_i(t;\rho_{opt})$ denote the transformed version of the original time-series $X_i(t)$ using the optimal value of ρ, ρ_{opt}. Fig. 9 shows the Box-Cox transformed version ($Y_3(t)$) of the original series $X_3(t)$, as well as, the mean and standard deviation per hour-of-day ($h(t) \in \{1,\ldots,24\}$) of the original series $X_3(t)$. It is apparent that the effect of the large spikes, present in $X_3(t)$, has been degraded in $Y_3(t)$. Besides, notice that $X_3(t)$ exhibits strong non-stationarity in both the mean and the standard deviation (see the two bottom plots in Fig. 9).

This analysis motivates us to further normalize the transformed time-series, $Y_i(t)$, in the following way:

$$G_i(t) = \frac{Y_i(t) - \mu_{i,h(t)}}{\sigma_{i,h(t)}}\ , \tag{11}$$

where $h(t)$ is the corresponding hour-of-day for time t, while $\mu_{i,h(t)}$ and $\sigma_{i,h(t)}$ are the mean and standard deviation of $Y_i(t)$ during those time periods with the hour-of-day being $h(t)$, respectively. Notice that the computation of $\mu_{i,h(t)}$ and $\sigma_{i,h(t)}$ depends on the periodicity of the measurements of the particular AP. In particular, when the AP has a diurnal periodicity (24 hours), $\mu_{i,h(t)}$ is the mean of the traffic measurements obtained at the same hour-of-day $h(t)$. Assume, for instance, that we want to normalize the measurements obtained at 11:00 a.m. for each day. Then, $\mu_{i,h(t)}$ is the mean of all the traffic measurements corresponding only to 11:00 a.m., where the mean is taken over all the days in our trace. On the other hand, we must be careful when the periodicity of an AP is not diurnal. For instance, assume that we want to normalize the measurements of an AP with a periodicity of 22 hours, obtained at 11:00 a.m. for each day. Then, $\mu_{i,h(t)}$ is the mean of all the traffic measurements corresponding to hours-of-day, whose difference is equal to 22 hours between adjacent days. The computation of the standard deviation, $\sigma_{i,h(t)}$, is performed in the same way.

It is also important to notice that after the above transformations, the model that best fits the empirical distribution of $G_i(t)$ and the optimal window length L, given by the sample auto-correlation function, may change.

4.3 Low-dimensionality of traffic load series

As described in Section 3.3, the energy contributed by each eigenload to the actual traffic load is concentrated in the first few leading components. Fig. 10 shows the percentage contribution of the eigenvalues for the normalized series $G_9(t)$, for the optimal window length $L = 33$, as well as the χ^2 test, where the null hypothesis is that the Weibull PDF is closer to the empirical distribution. According to the χ^2 test, only the first 6 principal components (out of the 33) are adequate to capture the vast majority of traffic variability, and thus, accurately approximate the original series $X_9(t)$. The first 6 principal components contribute in the 72.42% of the total energy of $G_9(t)$. Thus, the time-series $G_9(t)$ has a structure with effective dimension equal to 6, much lower than the total number of principal components (33). The χ^2 test is consistent with an energy-based rule, in the sense that, the few first principal components for which the χ^2 value falls inside the confidence interval, are exactly those components containing the highest portion of the total energy.

As a further illustration of this low-dimensionality property of the traffic load series, we plot the time-series $\hat{G}_9(t)$, which is reconstructed using the first 6 leading eigenloads. The results are shown in Fig. 11(a), while in Fig. 11(b) we plot the original series $X_9(t)$ and its approximation $\hat{X}_9(t)$, obtained after applying the inverse transforms of Eqs. (9), (11) (in this order). Notice that even though we omitted 27 principal components, we can still capture most of the important characteristics of the original series $X_9(t)$, such as the locations of its spikes. We do not expect to capture accurately the exact height of a spike, using only such a small number of eigenloads. Our goal is to illustrate that the main information content of a traffic load series in our dataset is mainly due to the contribution of a small number of features (eigenloads). Thus, we can understand better the intrinsic behavior of actual traffic by studying the behavior of a small set of eigenloads, which appear to have a better structure compared with the original traffic load series, as described in the next section.

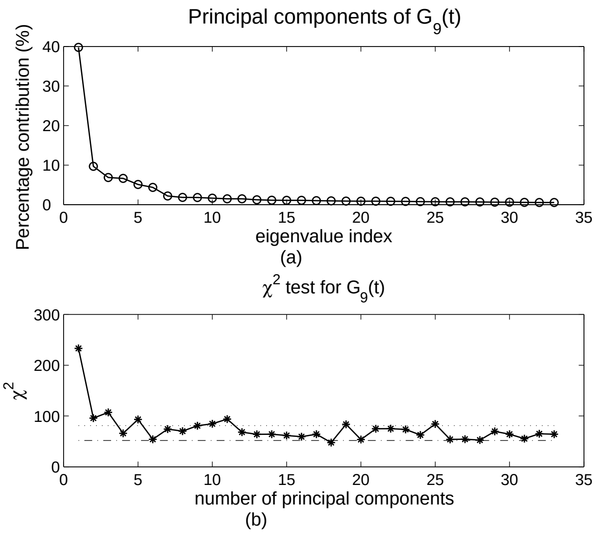

Figure 10: (a) Percentage contribution of the eigenvalues and (b) χ^2 test values for $G_9(t)$ ($L = 33$).

5. STRUCTURE OF THE EIGENLOADS

The statistical analysis of the traffic load series presented in the previous section underscores the central role of the eigenloads in understanding the intrinsic properties of a traffic load series obtained in a large-scale WLAN, such as the network considered in our study. Thus, we are interested in describing the two types of eigenloads, namely, the deterministic (slow-varying) and the noisy one.

5.1 Categorization of eigenloads

In Section 3.1, we defined the set of eigenloads $\{V_j\}_{j=1}^r$ as a function of the set of eigenpairs $\{\lambda_j, U_j\}_{j=1}^r$. The value of λ_j is proportional to the extend to which its corresponding principal component U_j contributes to the j-th eigenload of the time-series $X(t)$. Thus, before the categorization of the eigenloads, we start by inspecting the set of principal components $\{U_j\}_{j=1}^r$.

The principal components of the traffic load series in our dataset for each one of the 19 hotspot APs appear to have the same behavior. In particular, we found that a principal component whose corresponding eigenvalue is of high magnitude is slow-varying, whereas as the magnitude of an eigenvalue decreases, its corresponding eigenvector oscillates more and more. As an illustration of this behavior, Fig. 12 shows a subset of the principal components for the normalized series $G_9(t)$ and $G_{18}(t)$, where the principal components are ordered in decreasing order with respect to their corresponding eigenvalue.

The categorization of the set of eigenloads is performed in a heuristic way. In particular, we expect that the eigenloads will present a similar behavior as the principal components, since they are obtained as projections of the trajectory matrix $\mathbf{H}$ on them. Thus, we divide the eigenloads in two classes: (i) the deterministic, slow-varying eigenloads, which are simply the projections of $\mathbf{H}$ on slow-varying principal components, and (ii) the noisy eigenloads, which result by projecting $\mathbf{H}$ on the high-frequency principal components. As an example, Fig. 13 shows the eigenloads given by the projection of the trajectory matrix of the normalized time-

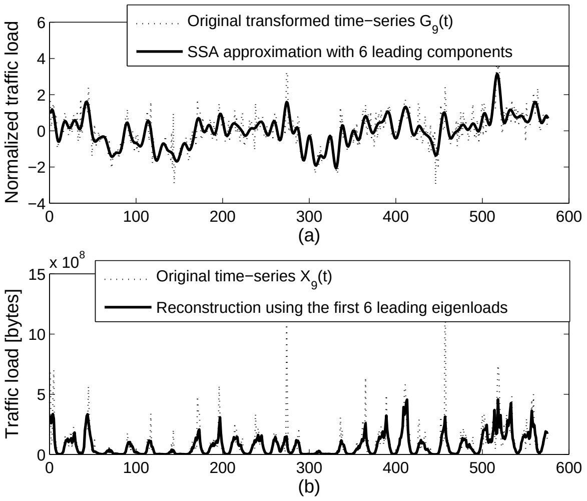

Figure 11: SSA approximation using the first 6 leading components for: (a) the normalized series $G_9(t)$, (b) the original series $X_9(t)$.

series $G_9(t)$ on the principal components 1, 5, 22 and 33. It is clear that the eigenloads 1 and 5 can be considered as deterministic, while the eigenloads 22 and 33 belong to the noisy class.

5.2 Decomposition of the traffic load series

A benefit of the above eigenload-based categorization is that it results in a decomposition of any given traffic load series (normalized or not) into its principal features. That is, we can reconstruct each time-series in terms of two constituents: the contributions made by the deterministic and the noisy eigenloads. Doing so, each constituent is responsible to capture a distinct feature of the traffic load series, namely, its deterministic mean and its (stationary) random variation, respectively. An example of this decomposition is shown in Fig. 14. The figure shows the original normalized traffic series $G_9(t)$ along with its four approximations based on the features captured by the first four eigenloads (i.e., the eigenloads corresponding to the first four leading components).

This decomposition may be very useful for the future design of a forecasting system, since the eigenloads which carry most of the information content of the original time-series are exactly the first few deterministic ones, which can be predicted more accurately because of their slow-varying behavior.

6. CONCLUSIONS

In this paper, we provided an SSA-based statistical analysis of the structure of traffic load series measured in a large-scale campus-wide WLAN. First, we fitted the distribution of a given traffic load series, obtained at the AP level, using an appropriate model selected from a set of pre-determined candidate PDFs. Then, we applied the SSA approach in order to partition the set of principal components in two subsets, namely, the subset of leading components and the subset of residual components.

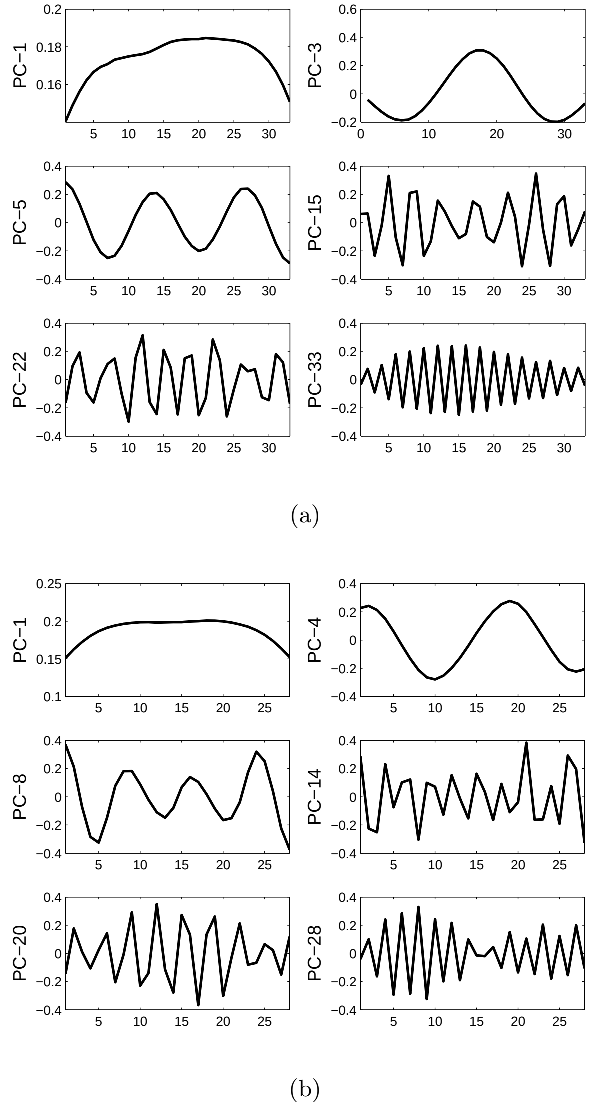

(a)

(b)

Figure 12: Principal components of the normalized time-series: (a) $G_9(t)$, (b) $G_{18}(t)$.

We showed that the subset of leading components is responsible for the preservation of the main information content of the original series and thus, the intrinsic dimensionality of the traffic is highly restricted by using only the first few leading components. Besides, we found that the eigenloads, defined using the set of leading components, present a similar behavior across the different traffic load series. In particular, we showed that they can be categorized in two classes: (i) the deterministic, slow-varying eigenloads carrying the major information content and (ii) the noisy eigenloads, which are related with the irregular variations of the traffic.

Based on this categorization, we decomposed the original traffic series by projecting it on each eigenload. This yielded a considerable understanding of the structure of the traffic load series, which is analyzed in multiple frequency scales, since the projections on the first eigenloads give the slow-

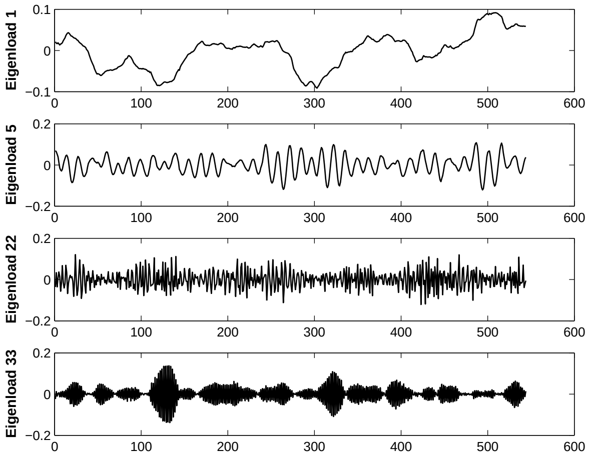

Figure 13: Eigenloads of the traffic load series $G_9(t)$.

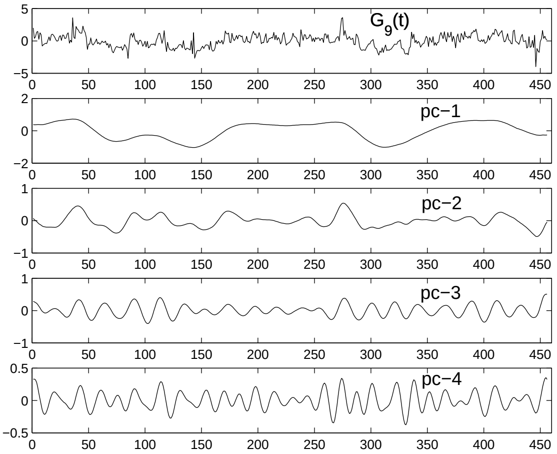

Figure 14: Original normalized traffic load series $G_9(t)$ along with its approximations based on the first four eigenloads.

varying trend components, while the projections on the last eigenloads give the high-frequency content.

As a future work, we will use the statistical analysis and the SSA-based decomposition to design a forecasting algorithm, by exploiting efficiently the characteristics of the eigenloads. Besides, to encourage further experimentation, we have made our datasets available to the research community [19].

7. REFERENCES

[1] T. Henderson, D. Kotz, and I. Abyzov, "The changing usage of a mature campuswide wireless network", *In ACM/IEEE International Conference on Mobile Computing and Networking (MobiCom)*, Philadelphia, Sep. 2004.

[2] M. Ploumidis, M. Papadopouli, and T. Karagiannis, "Multi-level application-based traffic characterization in a large-scale wireless network", *in Proc. of the IEEE International Symposium on a World of Wireless, Mobile and Multimedia Networks (WoWMoM)*, Helsinki, Finland, June 2007.

[3] F. Anjum, et al., "Voice performance in WLan networks, an experimental study", *in Proc. of the IEEE Conference on Global Communications (GLOBECOM)*, Rio De Janeiro, Brazil, Dec. 2003.

[4] W. E. Leland, M. S. Taqqu, W. Willinger, and D. V. Wilson, "On the self-similar nature of ethernet traffic", *ACM Computer Communication Review*, 25(1):202Ű-213, 1995.

[5] W. E. Leland, W. Willinger, M. S. Taqqu, and D. V. Wilson, "Statistical analysis and stochastic modeling of self-similar datatraffic", *in Proc. 14th Int. Teletraffic Cong.*, Vol. 1, pp 319-Ű328, Antibes Juan Les Pins, France, June 1994.

[6] A. Lakhina, K. Papagiannaki, M. Crovella, C. Diot, E. .D. Kolaczyk, and N. Taft, "Structural Analysis of Network Traffic Flows", *ACM Sigmetrics*, New York, June 2004.

[7] F. H. Campos, M. Karaliopoulos, M. Papadopouli, and H. Shen, "Spatio-Temporal Modeling of Traffic Workload in a Campus WLAN", *2nd annual intl. WIreless internet CONference (WICON'06)*, Boston, USA, August 2-5, 2006.

[8] M. Karaliopoulos, M. Papadopouli, E. Raftopoulos, and H. Shen, "On scalable measurement-driven modelling of traffic demand in large WLans", *in Proc. of the IEEE Workshop on Local and Metropolitan Area Networks*, Princeton NJ, USA, June 10-13, 2007.

[9] M. Papadopouli, H. Shen, E. Raftopoulos, M. Ploumidis, and F. Hernandez-Campos, "Short-term traffic forecasting in a campus-wide wireless network", *16th Annual IEEE Intl. Symp. on Personal Indoor and Mobile Radio Comm.*, Berlin, Germany, September 11-14, 2005.

[10] M. Papadopouli, E. Raftopoulos, and H. Shen, "Evaluation of short-term traffic forecasting algorithms in wireless networks", *2nd Conf. on Next Generation Internet Design and Engineering*, Valencia, Spain, April 3-5, 2006.

[11] America's most connected campuses. `http://forbes.com/home/lists/2004/10/20/04conncampland.html`.

[12] H. D. I. Abarbanel, *"Analysis of Observed Chaotic Data"*, Springer-Verlag New York, Inc., 1996.

[13] I. T. Jolliffe, *"Principal Component Analysis"*, Springer-Verlag, 1986.

[14] N. Golyandina, V. Nekrutkin, and A. Zhigljavsky, *"Analysis of Time Series Structure: SSA and Related Techniques"*, Chapman & Hall/CRC, 2001.

[15] I. Antoniou, et al., "Principal Component Analysis of Network Traffic Measurements: the "Caterpillar"-SSA approach", *"VIII Int. Workshop on Advanced Computing and Analysis Techniques in Physics Research, ACAT'2002*, 24-28 June 2002, Moscow Russia.

[16] M. H. Hayes, *"Statistical Digital Signal Processing and Modeling"*, John Wiley & Sons, 1996.

[17] P. E. Greenwood and M. S. Nikulin, *"A Guide to Chi-Squared Testing"*, J. Wiley & Sons Canada, Ltd., 1996.

[18] G. E. P. Box, G. M. Jenkins, and G. C. Reinsel, *"Time Series Analysis, Forecasting and Control"*, 3rd ed. Prentice Hall, Englewood Clifs, NJ, 1994.

[19] UNC/FO.R.T.H. archive of wireless traces, models and tools. `http://netserver.ics.forth.gr/datatraces/`